AGU PUBLICATIONS

JGR

Journal of Geophysical Research: Atmospheres

RESEARCH ARTICLE
10.1002/2015JD023772

Key Points:
- A new physically based multiscalar drought index (SZI) was developed
- The SZI has a multiscalar character that is lacking in the PDSI
- The SZI provides more reasonable estimation of water demand than SPEI

Correspondence to:
P. Wu and J. Jin,
gjzwpt@vip.sina.com;
jimingjin99@gmail.com

Citation:
Zhang, B., X. Zhao, J. Jin, and P. Wu (2015), Development and evaluation of a physically based multiscalar drought index: The Standardized Moisture Anomaly Index, *J. Geophys. Res. Atmos.*, *120*, 11,575–11,588, doi:10.1002/2015JD023772.

Received 9 JUN 2015
Accepted 4 NOV 2015
Accepted article online 6 NOV 2015
Published online 27 NOV 2015

Development and evaluation of a physically based multiscalar drought index: The Standardized Moisture Anomaly Index

Baoqing Zhang[1,2,3], Xining Zhao[1], Jiming Jin[1,3], and Pute Wu[1]

[1]College of Water Resources and Architectural Engineering, Institute of Water Saving Agriculture in Arid Regions of China, Northwest A&F University, Yangling, China, [2]Key Laboratory of Western China's Environmental Systems (Ministry of Education), College of Earth and Environmental Sciences, Lanzhou University, Lanzhou, China, [3]Departments of Watershed Sciences and Plants, Soils, and Climate, Utah State University, Logan, Utah, USA

Abstract In this study, a new physically based multiscalar drought index, the Standardized Moisture Anomaly Index (SZI), was developed and evaluated, which combines the advantages of the Palmer Drought Severity Index (PDSI) and the Standardized Precipitation Evapotranspiration Index (SPEI). The SZI is based on the water budget simulations produced with a sophisticated hydrological model, and it also includes a multiscalar feature to quantify drought events at different temporal scales taken from SPEI. The Chinese Loess Plateau was selected to evaluate the performance of the SZI. Our evaluation indicates that the SZI accurately captures the onset, duration, and ending of a multiyear drought event through its multiscalar feature, while the PDSI, which lacks this feature, is often unable to describe the evolution of a multiyear drought event. In addition, the variability of the SZI is more consistent with observed streamflow and the satellite normalized difference vegetation index than that of the Standardized Precipitation Index and the SPEI. Although the SPEI includes potential evapotranspiration (PE) as water demand, water demand is often unrealistically estimated based solely on PE, especially over arid and semiarid regions. The improved drought quantification with the SZI is the result of a more reasonable estimation of water demand by including evapotranspiration, runoff, and any change in soil moisture storage. In general, our newly developed SZI is physically based and includes a multiscalar feature, which enables it to provide better information for drought monitoring and identification at different temporal scales.

1. Introduction

Drought is recognized as one of the costliest natural disasters in the world [*Wilhite*, 2000], resulting in 55% of the economic losses caused by natural disasters [*Zhai et al*., 2005, 2010]. Based on an analysis of precipitation, streamflow, and drought indices, *Dai* [2011, 2013] indicated that the area of global drought has increased significantly since 1950 in many regions. Northern China, as the largest drought-prone region, experienced severe droughts during the second half of the twentieth century, and the most severe and prolonged droughts have occurred since 1990 [*Zou et al*., 2005; *Zhai et al*., 2010]. In 1997, a severe drought occurred in the Yellow River basin, the largest river in northern China, resulting in a streamflow disruption at its outlet for a period of 226 days, which was the longest in recorded history [*Zou et al*., 2005]. The 2008/2009 winter drought in the Huang-Huai-Hai River basin in northern China was one of the worst in the past 50 years, causing an estimated 2.3 billion U.S. dollars in economic loss and subjecting more than 10 million people to water scarcity [*A. H. Wang et al*., 2011]. Thus, monitoring, understanding, and predicting drought events are essential to the well-being of northern China.

Drought is a complex climate phenomenon that results mainly from a long-term deficiency in precipitation [*Yuan and Quiring*, 2014]. It is defined in several different ways in terms of applications. For example, a simple precipitation deficiency is commonly referred to as meteorological drought; hydrological drought is caused mainly by the lack of surface water and groundwater; and agricultural drought results primarily from low levels of soil moisture [*Sheffield et al*., 2004; *Sheffield and Wood*, 2007; *Vicente-Serrano and López-Moreno*, 2005; *Wang et al*., 2009; *Hao and AghaKouchak*, 2013; *Rajsekhar et al*., 2015]. These different definitions make it difficult to objectively quantify drought features such as magnitude, duration, and spatial extent [*Dai et al*., 2004; *Vicente-Serrano et al*., 2011, 2012]. Drought indices are a common way to identify drought events, and development of such an index for varied applications is essential to water resource prediction

and management [*Palmer*, 1965]. In recent years, attempts have been made to develop and evaluate different drought indices to quantitatively account for various drought characteristics [*Wells et al*., 2004; *Vicente-Serrano et al*., 2010; *Xu et al*., 2012; *Hao and AghaKouchak*, 2013; *Mu et al*., 2013; *Rajsekhar et al*., 2015]. However, it is still difficult to establish a universal drought index that can monitor and identify all kinds of drought [*Carbone et al*., 2008]. Two prominent drought indices that have been widely used in climate and hydrology studies are (1) the Palmer Drought Severity Index (PDSI) [*Palmer*, 1965], based on the water balance equation, and (2) the Standardized Precipitation Index (SPI) [*McKee et al*., 1993], based on a probabilistic precipitation approach.

The PDSI uses a water balance model to compute the cumulative moisture departure on the land surface. It incorporates antecedent and current moisture supply and demand into a hydrological budget system based on a simple two-layer bucket model. Here water supply is defined as precipitation, and water demand is evapotranspiration, runoff, and any changes in soil moisture storage. In the computation of the PDSI, an intermediate term is defined, called the moisture anomaly index (Z), which is used to calculate the surface moisture anomaly for the current month [*Dai et al*., 2004]. Although the PDSI is a physically based index, it still has several drawbacks, including mainly (1) the use of an oversimplified two-layer bucket-type hydrological model that often unrealistically simulates the water balance components, (2) a strong calibration influence that often generates unrepresentative model parameters, and (3) fixed temporal scales [*Alley*, 1984; *Wells et al*., 2004; *Vicente-Serrano et al*., 2012; *Zhang et al*., 2012].

The PDSI uses a two-layer bucket-type model that is based primarily on an empirical water balance equation and does not consider the impacts of complex topography and the spatial heterogeneity of soil and vegetation on the hydrological processes in a watershed [*Xu et al*., 2012]. *Zhang et al*. [2012, 2014] used the Variable Infiltration Capacity (VIC) model [*Liang et al*., 1994] to replace the two-layer bucket-type model in the PDSI calculations and established a physically based Palmer drought index (VIC-PDSI), which provides an improved hydrological budget for the PDSI. In addition, the self-calibrated PDSI (sc-PDSI), developed based on the original PDSI, can generate more representative model parameters at temporal and spatial scales [*Wells et al*., 2004; *Todd et al*., 2013]. However, as reported by *Vicente-Serrano et al*. [2011, 2012], the PDSI still lacks the ability to identify drought events within a watershed at multiple timescales.

To improve on the PDSI drawback of a fixed temporal scale, a multiscalar drought index, the SPI, has been used to take into account the characteristics of drought at temporal scales varying from 1 month to several years [*McKee et al*., 1993]. It allows users to examine wet and dry spells over a range of timescales. However, the main limitation of the SPI is that it is based on precipitation (P) and ignores the effects of atmospheric water demand [*McEvoy et al*., 2012; *Shi et al*., 2014]. In an effort to improve the SPI, *Vicente-Serrano et al*. [2010] recently developed the Standardized Precipitation Evapotranspiration Index (SPEI), which accounts for both water supply and demand and uses the difference between P and potential evapotranspiration (PE) to evaluate the water deficit or surplus. Similar to the SPI, the calculation of the SPEI is also based on a probabilistic moisture approach, which enables its multiscalar characteristic. The SPEI represents a more physically based estimate of dynamic drought severity compared to SPI, particularly in regions that have experienced significant drying and warming over the last century, and the SPEI and sc-PDSI show a high correlation [*Vicente-Serrano et al*., 2010; *McEvoy et al*., 2012]. However, the PE is not the only variable that affects the water demand and thus drought conditions, while the surface runoff and soil moisture storage also play important roles in estimating the water demand [*Palmer*, 1965].

As described by *Palmer* [1965], a required amount of precipitation that is climatically appropriate for existing conditions (CAFEC, defined as $\widehat{P}$) is computed in the PDSI to estimate water demand. When the amount of actual P is equal to $\widehat{P}$, the local water will remain normal, without a deficit or surplus. As a result, the difference between the actual and CAFEC precipitation is a good indicator of water deficiency or surplus; it is called moisture departure and is expressed as $d = P - \widehat{P}$ [*Wells et al*., 2004]. The calculation of $\widehat{P}$ includes precipitation, soil moisture loss and recharge, runoff, and evapotranspiration, and all these variables can affect surface water balance and thus drought conditions, whereas PE considers only atmospheric demand for water. In addition, a weighing factor in the PDSI called the climatic characteristic, K_j, is defined as the ratio between the long-term averaged water demand and supply [*Palmer*, 1965], which is a measure of the local significance of moisture departure. The moisture departure, d, is then converted

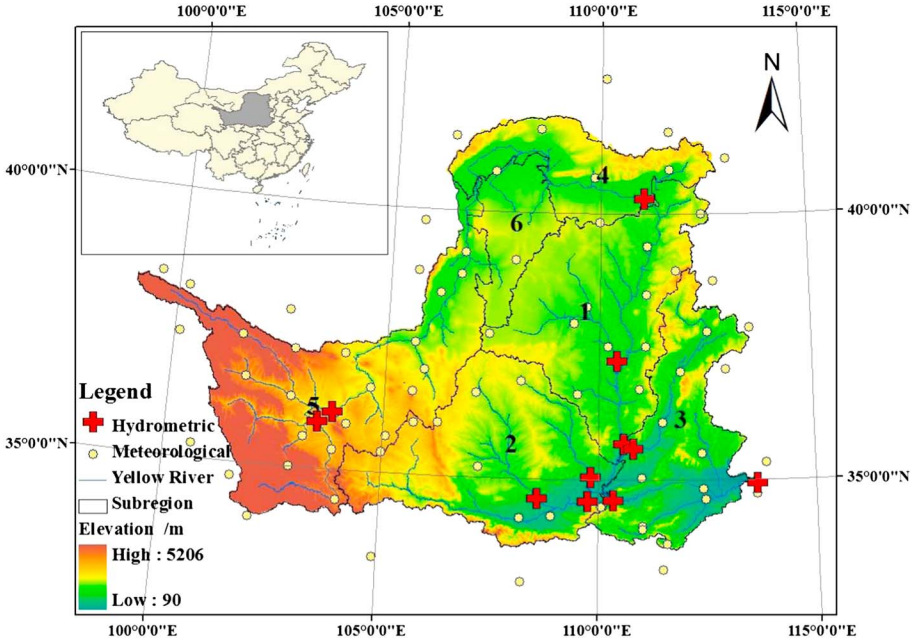

Figure 1. Spatial distributions of the hydrometric and meteorological stations over six subregions of the Loess Plateau.

into the Palmer moisture anomaly index as $Z = K_j d$, which is used to characterize the moisture anomaly condition for a single month. Since it takes all components of the surface water balance into account, Z is a more realistic moisture deficit or surplus indicator than the difference between P and PE in the SPEI. Therefore, the objective of this study is to develop and evaluate a new physically based multiscalar drought index, the Standardized Moisture Anomaly Index (SZI), which is formulated based on the Z value from the PDSI and the probabilistic moisture approach of the SPEI. This new drought index combines the strengths of both the PDSI and SPEI. This paper is arranged as follows: Section 2 focuses on the study area and introduces the data and SZI development, section 3 includes our index evaluation results and discussion, and the conclusion is given in section 4.

2. Study Area, Data, and Methodology

2.1. Study Area

The Loess Plateau in northern China, one of the driest areas in the world, was selected as our drought index evaluation area. This plateau covers an area of approximately 6.4×10^5 km^2 and is traversed by the upper and middle reaches of the Yellow River (Figure 1). The plateau is 1000–1600 m above sea level and is part of the Asian monsoon region. The annual average temperature over the northwest portion of the plateau is 4.3°C and 14.3°C in its southeast portion [*Zhang et al.*, 2013]. The annual precipitation ranges from 200 mm in the northwest to 800 mm in the southeast. The unevenly distributed rainfall is one of the main reasons that the plateau is vulnerable to drought. Precipitation events concentrate mainly from June to September, accounting for approximately 70% of the total annual precipitation, with much of it coming in the form of high-intensity storms [*Y. Q. Wang et al.*, 2011]. Most water from heavy rainstorms becomes high surface runoff (because of insufficient soil infiltration), often causing significant drought conditions in the soil [*Brocca et al.*, 2010, 2014]. Thus, the Loess Plateau was chosen as our study region to examine the performance of different drought indices.

The Loess Plateau includes arid, semiarid, and semihumid climate zones, and these different zones help provide a clear understanding of the performance of drought indices. Following previous research [*Yan and Xu*, 2007], the Loess Plateau in this study was also divided into six subregions, based on the completeness of the drainage area and the similarity in precipitation patterns, vegetation cover, and geographical conditions (Figure 1). These subregions are, respectively, located in semiarid (subregions 1 and 5), semihumid (subregions 2 and 3), and arid (subregions 4 and 6) climate zones [*Zhang et al.*, 2012].

2.2. Data

The meteorological forcing data for driving the VIC model with a daily step came from 73 meteorological stations in the Loess Plateau and its surrounding area for the period of 1971 through 2012, including daily precipitation, maximum and minimum air temperatures, solar radiation, relative humidity, pressure, and wind speed. These observed data were obtained from the Data and Information Center of the China Meteorological Administration (http://data.cma.gov.cn/site/index.html). In addition, these observed meteorological forcing data were also used to calculate the SPI and SPEI.

Running the VIC model requires three types of user-defined parameters: soil, vegetation, and watershed definitions. The soil parameters of the VIC model were obtained from the global 10 km soil profile data set provided by the National Oceanic and Atmospheric Administration (NOAA) hydrology office [*Reynolds et al*., 2000]. The VIC vegetation parameters, including architectural resistance, minimum stomata resistance, leaf area index, albedo, roughness length, and zero-plane displacement, were obtained from the Land Data Assimilation System at 1 km resolution [*Hansen et al*., 2000]. A digital elevation model (DEM) data set was obtained from the advanced spaceborne thermal emission and reflection radiometer global digital elevation model (http://gdem.ersdac.jspacesystems.or.jp/), with a spatial resolution of 30 m, to delineate the boundaries of the basin in the VIC model. These DEM data were also used to identify the channel networks, water flow direction, and other features in the watershed.

The observed monthly hydrologic data from 11 key gauge stations along the Yellow River were from the Hydrology Bureau of the Yellow River Conservancy Commission of China (http://www.hwswj.gov.cn/swjcms/index.jsp). These data were used to calibrate and validate the VIC model. In order to minimize the impact of soil and water conservation measures, large reservoirs, and dams, the observed hydrological data from Hongqi and Huaxian stations were chosen to analyze the relationships between drought indices and river runoff, where few human disturbances are found [*Xin et al*., 2011]. The Climate Prediction Center (CPC) monthly soil moisture data set was used to evaluate the performance of the VIC model in simulating the soil water content (http://www.esrl.noaa.gov/psd/data/gridded/data.cpcsoil.html). The Normalized Difference Vegetation Index (NDVI) data, which were used to evaluate the performance of different drought indices, were from the NOAA advanced very high resolution radiometer land data set at a spatial resolution of 8 km at 15 day intervals from January 1982 to December 2006 [*Myneni et al*., 2001; *Tucker et al*., 2005]. Figure 1 shows the spatial distributions of the hydrometric and meteorological stations as well as the topography of the Loess Plateau.

2.3. Methodology

2.3.1. SPI, SPEI, and VIC-PDSI Calculations

In this study, we calculated the SPI and SPEI in order to compare them with our newly developed SZI. The SPI was computed using solely monthly P as the input data. This index does not take water demand into account and therefore neglects other physical processes that drive drought dynamics. The SPEI calculation was made with the monthly difference (D) between P and PE, though using the Penman-Monteith equation [*Allen et al*., 1998] to generate the PE often overestimates water demand, especially in arid and semiarid regions, as mentioned previously. This overestimation can lead to flawed drought identification. In this study, the PE in the SPEI was generated with the Penman-Monteith equation [*Allen et al*., 1998]. For calculating the SPI at different timescales, a two-parameter gamma distribution was used by *McKee et al*. [1993]. However, a three-parameter distribution is needed for computing the SPEI at different timescales. In the two-parameter distributions, the variable, such as P, has a lower boundary of zero, whereas the D series used in the SPEI often has negative values, which require the three-parameter distribution [*Vicente-Serrano et al*., 2010]. That means the three-parameter distribution can be used to calculate both the SPI and the SPEI. *Vicente-Serrano et al*. [2010] tested various probability distributions and finally selected the three-parameter log-logistic distribution for calculating the SPEI. Detailed calculation information for the SPEI can be found in *Vicente-Serrano et al*. [2010, 2011]. In order to facilitate comparison, the SPI was also generated by the log-logistic distribution in this study. The calculation procedure of the VIC-PDSI is similar to that of the original PDSI [*Palmer*, 1965]. However, the hydrological budget in the VIC-PDSI is based on the simulation results of the VIC model, while the hydrological budget in the original PDSI is based on the results of the two-layer bucket model, as discussed above. The detailed computation procedure of the VIC-PDSI is included in *Zhang et al*. [2012, 2014]. With the methods described above, the SPI, SPEI, and VIC-PDSI over the Loess Plateau from 1971 to 2012 were derived in this study.

2.3.2. Development of the Standardized Moisture Anomaly Index

2.3.2.1. Simulations of Hydrological Processes

In this work, version 4.1.1 of VIC was used to reconstruct daily water balance components and soil moisture values at a spatial resolution of 50 km, covering the entire Loess Plateau from 1 January 1971 to 31 December 2012. Due to the limited coverage of observed meteorological data, the model is incapable of running at a very fine resolution over the Loess Plateau [*Wu et al*., 2011; *Wang et al*., 2012]. However, our results are reasonable when compared with observations (discussed in section 2.3.3), implying that the 50 km resolution data are still able to capture the main features of hydrological processes in this region of complex terrain. Since the VIC model uses a grid-based modeling approach, the meteorological forcing fields for each station were interpolated using an inverse distance weighting method into 50 km × 50 km grids [*Wu et al*., 2007, 2011].

The VIC model divides the soil profile of the study area into three layers. The upper two soil layers of the model are designed to represent the dynamic response of soil to rainfall events, and the bottom layer is used to characterize the behavior of seasonal soil moisture. To match the calculation of the SZI, where the soil column is divided into two layers, the upper two soil layers in VIC were combined, leaving the bottom layer. A similar method was used in *Wu et al*. [2007, 2011] and *Wang et al*. [2012].

Three types of evaporation in VIC were considered: (1) evaporation from the canopy layer (E_c, mm) of each vegetation type, (2) transpiration (E_t, mm) from each vegetation type, and (3) evaporation from the bare soil (E_1, mm) [*Liang et al*., 1994; *Xie et al*., 2007; *Dan et al*., 2012]. The total evapotranspiration over a grid cell was computed as the sum of these three components.

The Nash-Sutcliffe efficiency (NSE) coefficient was employed to calibrate and validate the model. The NSE is a normalized statistic reflecting the relative magnitude of the residual variance compared to the measured data variance [*Nash and Sutcliffe*, 1970; *Wang et al*., 2012]. The NSE ranges between $-\infty$ and 1, and the greater it is, the better the simulation results are. When the NSE is greater than 0.75, the simulation results are usually regarded as acceptable [*Nash and Sutcliffe*, 1970; *Wang et al*., 2012].

There are seven hydrological parameters in the VIC model that need to be calibrated with observed streamflow. The observed streamflows from 11 key hydrometric stations were divided into two groups: (1) Lanzhou, Toudaoguai, Longmen, Tongguan, Huayuankou, and Huaxian for model calibration (these stations are located in the mainstream of the Yellow River) and (2) Hongqi, Baijiachuan, Hejin, Zhangjiashan, and Zhuangtou for model validation (these stations are located in the tributaries of the Yellow River). Figure 2 shows the relationship between observed and simulated annual streamflow over the six calibration and five validation hydrometric stations on the Loess Plateau. The annual streamflow simulations at all 11 hydrometric stations closely matched the observed values, wherein the NSEs ranged between 75.5% and 91.8%, which are all greater than 75%. However, the VIC model overestimated some peak flows. These errors could possibly be attributed to human soil and water conservation measures on the Loess Plateau, including check dams, fish-scale pits, and bench terraces, which tend to reduce the peak flows.

It is known that soil moisture is crucial for deriving drought indices such as the PDSI or the SZI. However, it is one of the least observed variables of the hydrologic cycle in terms of long-term and large-scale measurements [*Sheffield et al*., 2004]. Moreover, the representativeness of point measurements of soil moisture for regional applications is often questioned due to high spatial heterogeneity [*Prigent et al*., 2005; *Mishra and Singh*, 2010]. *Mishra and Singh* [2010] and *Mishra et al.* [2015] indicated that the drought indices derived from soil moisture lacks quality data, and quantification of soil moisture supply in the root zone remains a gray area in the research community of drought. There is a substantial lack of large-scale and long-term in situ observations of soil moisture [*Sheffield et al*., 2004; *A. H. Wang et al*., 2009, 2011]. In addition, the satellite soil moisture data have an excellent spatial coverage, but their quality is still in question especially for the lower soil depths [*Brocca et al*., 2014]. Thus, validation of the model-simulated soil moisture with observations for our study region is difficult. However, variations of soil moisture are highly correlated with those of precipitation for a long term [*Brocca et al*., 2014], and the latter are much better observed. Thus, some soil moisture reanalysis products that are driven by observed precipitation are useful in evaluating soil moisture variations. In this study, the CPC soil moisture reanalysis data were used to examine the simulated soil moisture anomalies over the Loess Plateau.

A comparison of CPC and VIC-simulated soil moisture over the Loess Plateau demonstrates that the VIC model produces generally higher soil water content than CPC during the whole study period, but it captures the spatiotemporal variations of soil moisture reasonably well (figure not shown). The mean CPC soil moisture

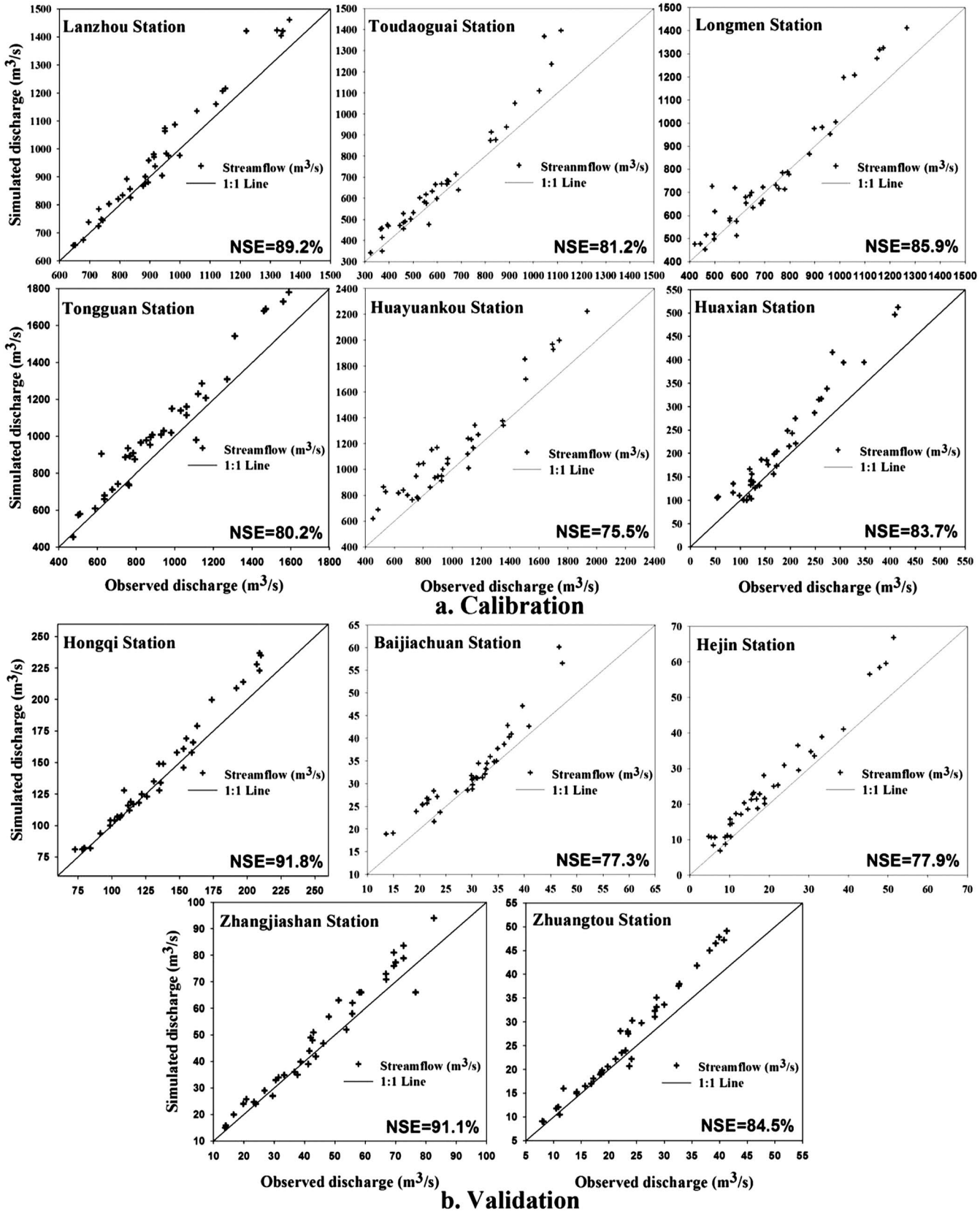

Figure 2. Comparison of the observed and simulated annual discharge (m^3/s) over six calibration and five validation hydrometric stations during 1971–2008 on the Loess Plateau.

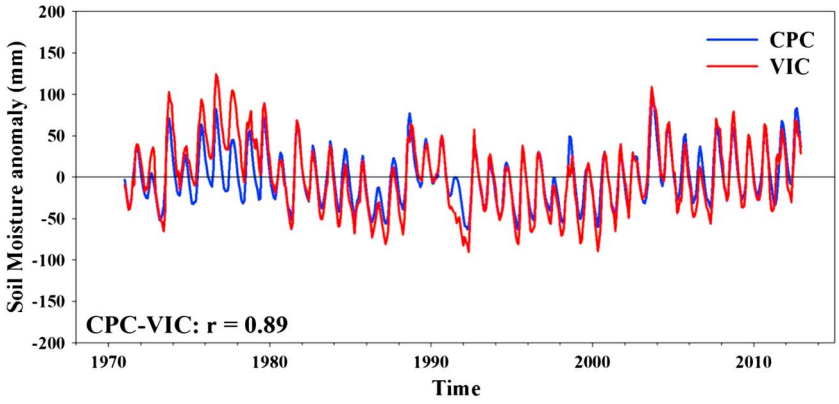

Figure 3. Time series of area-averaged monthly soil moisture anomalies (1 m) from CPC and the VIC model during 1971–2012 over the Loess Plateau.

is around 190 mm over the study region, which is about 20% lower than the VIC-simulated soil moisture. Although the magnitude of CPC soil moisture is different from that of the VIC-simulated soil moisture, it is the soil moisture anomaly, not its absolute magnitude, which affects the changes in dry and wet spells. Figure 3 shows the time series of area-averaged soil moisture anomalies from CPC and the VIC model over the Loess Plateau. It is seen that the VIC soil moisture anomalies agree well with the CPC soil moisture anomalies over the past four decades, and the Pearson correlation coefficient between VIC and CPC soil moisture anomalies is 0.89 (above the 99% significance level). Thus, the VIC model can provide reasonable hydrological variables over the Loess Plateau, and these are used in the calculation of the SZI.

2.3.2.2. The Hydrological Budget

As with the PDSI, the second step in establishing the SZI is to compute the monthly hydrological budget. Each month of the year, four water balance components related to the soil moisture were computed, along with their potential values. These values are evapotranspiration (ET), moisture recharge (*R*), surface runoff (RO), moisture loss (*L*), potential evapotranspiration (PE), potential recharge (PR), potential runoff (PRO), and potential moisture loss (PL). The specific calculation methods of the above values are discussed in *Zhang et al*. [2014].

2.3.2.3. Climatic Coefficients and $\widehat{P}$

In this study, the monthly climatic coefficients were computed as the ratios of the monthly climatic averages of actual to potential values, including the evapotranspiration coefficient (α_j), recharge coefficient (β_j), runoff coefficient (γ_j), and loss coefficient (δ_j):

$$\begin{cases} \alpha_j = \overline{\mathrm{ET}_j}/\overline{\mathrm{PE}_j} \\ \beta_j = \overline{R_j}/\overline{\mathrm{PR}_j} \\ \gamma_j = \overline{\mathrm{RO}_j}/\overline{\mathrm{PRO}_j} \\ \delta_j = \overline{L_j}/\overline{\mathrm{PL}_j} \end{cases} \tag{1}$$

where *j* ranges over the months of a year (i.e., $j = 1$–12). Each grid cell has the same climatic coefficients for the same month of different years [*Palmer*, 1965]. The derived climatic coefficients can be used to determine the amount of $\widehat{P}$:

$$\widehat{P} = \alpha_j \mathrm{PE} + \beta_j \mathrm{PR} + \gamma_j \mathrm{PRO} - \delta_j \mathrm{PL} \tag{2}$$

$\widehat{P}$ more realistically estimates the water demand than PE [*Palmer*, 1965].

2.3.2.4. Climatic Characteristic and Moisture Anomaly Index

The difference between the actual precipitation and $\widehat{P}$ is an indicator of the water deficit or surplus, expressed as follows:

$$d = P - \widehat{P} \tag{3}$$

These moisture departures (*d*) are converted into a moisture anomaly index (*Z*),

$$Z = K_j d \tag{4}$$

Table 1. The Drought or Wet Threshold Levels of the SZI, SPEI, and SPI

SZI, SPEI, and SPI	Drought Classification	SZI, SPEI, and SPI	Wet Classification
−2.0 or less	Extreme drought	2.0 or larger	Extreme wet spell
−1.50 to −1.99	Severe drought	1.50 to 1.99	Severe wet spell
−1.00 to −1.49	Moderate drought	1.00 to 1.49	Moderate wet spell
−0.50 to −0.99	Mild drought	0.50 to 0.99	Mild wet spell
0 to −0.49	Normal	0 to 0.49	Normal

where K_j, called the climatic characteristic, is a measure of the local significance of moisture departures and is computed as follows:

$$K_j = \left(\overline{\mathrm{ET}_j} + \overline{R_j}\right)/\left(\overline{P_j} + \overline{L_j}\right) \tag{5}$$

The Z value plays a very important role in measuring the moisture deficit or surplus in the SZI and is regarded as a better indicator of surface water deficit or surplus than the difference between P and PE in the SPEI.

2.3.2.5. Standardizing the *Z* Series to Obtain the SZI

The calculated Z values were aggregated at different timescales, following the same procedure as that for the SPEI [*Vicente-Serrano et al*., 2010]. Because both the D and Z series can be negative (i.e., they have a similar range), the three-parameter log-logistic distribution is capable of adopting different shapes to simulate the frequencies of both the D and Z series [*Vicente-Serrano et al*., 2010]. Therefore, the log-logistic distribution was selected to standardize the Z series and finally to derive the SZI at different timescales. The average value of the SZI is 0, and the standard deviation is 1. The SZI is a standardized variable, and it can therefore be compared with other standardized drought indices over time and space. Because they use the same probability distribution and the same standardizing methods, the drought threshold levels of the SZI, SPEI, and SPI are exactly the same [*McKee et al*., 1993; *Vicente-Serrano et al*., 2010], as shown in Table 1.

2.3.3. Evaluation of the SZI

In order to evaluate the performance and ability of the SZI, the drought identification results were compared with the VIC-PDSI and the other two most widely accepted multiscalar drought indices, the SPI and SPEI. As reported by previous studies [*McEvoy et al*., 2012; *Mu et al*., 2013], vegetation cover and streamflow are very sensitive to moisture availability and climate warming. Therefore, the correlations between vegetation cover and moisture availability, as well as the relationships between streamflow and drought variations, were selected as the evaluation criteria for the performance and ability of each drought index. The results presented herein are expected to provide a new method for drought identification and to lend scientific support to decision makers when formulating drought management policies to alleviate the adverse effects of drought.

3. Results and Discussion

3.1. The Advantages of the SZI Over VIC-PDSI

In this section, the SZI is compared with the VIC-PDSI over the Loess Plateau. Figure 4 shows the evolution of dry-wet spells during 1971–2012 on the Loess Plateau as characterized by the SZI and VIC-PDSI, respectively. The VIC-PDSI is calculated at monthly scales, while the SZI is generated at monthly, 12 month, 24 month, 36 month, and 48 month intervals, respectively, to monitor the drought and wet variations over different temporal scales. Both the SZI and VIC-PDSI can identify the drought and wet spells at monthly scales. However, the multiscalar character of a drought index is very important for drought monitoring and water resource management [*McKee et al*., 1993; *Hayes et al*., 1999]. A long-term averaged low precipitation can produce a severe drought with a long duration, but some individual high-precipitation events during this period may produce short wet spells in certain months. If we use the VIC-PDSI to characterize a multiyear drought event, the time-averaged value of VIC-PDSI is needed. However, the time-averaged VIC-PDSI is also influenced by the individual wet events, which may weaken the severity of the long-term drought and result in misleading information for water resource management.

For example, over the 48 month period of 1999–2002, averaged precipitation is 12% less than its climatology on the Loess Plateau, as shown in Figure 5a. Thus, such anomalously low precipitation results in the most severe drought over a 42 year period (1971–2012). This severe drought event is clearly identified by the 48 month scale of SZI, with an average value of −1.61 (red line in Figure 5b; SZI values between −1.50 and

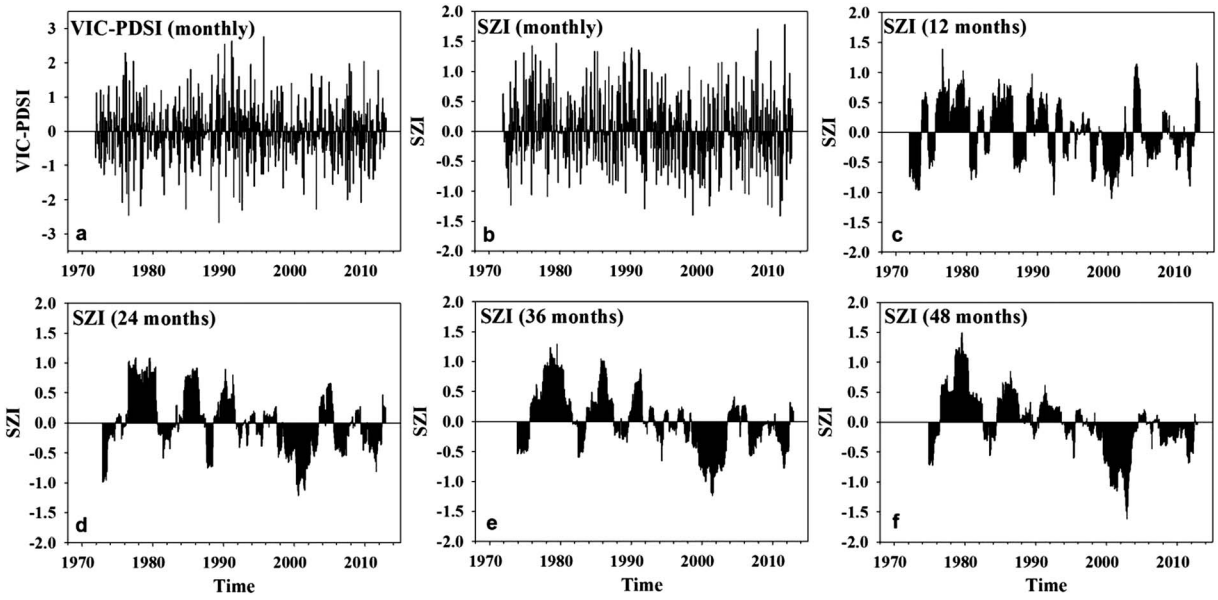

Figure 4. Comparisons of the SZI and VIC-PDSI over 1971–2012 on the Loess Plateau.

−1.99 are defined as severe drought). This index also accurately captures the onset, duration, and ending of the drought event, as shown in Figure 5b. Based on the 48 month SZI, about 30% of the total area of the Loess Plateau suffers from extreme drought over 1999–2002 (the averaged SZI in these regions is −2.11), and about half of its area has severe drought over the same period (the averaged SZI in these regions is −1.79). However, Figure 5b shows that the VIC-PDSI never captures the temporal evolution of this multiyear drought event. The time-averaged VIC-PDSI value from 1999 to 2002 is only −0.93, indicating that it is a very mild drought, even with some wet events included (VIC-PDSI values between −0.50 and −0.99 are defined as incipient drought). Based on the time-averaged VIC-PDSI, there is no region that suffers from severe or extreme drought. Therefore, the multiscalar character of the SZI has a strong advantage over the VIC-PDSI in quantifying drought for water resource management.

3.2. The Advantages of the SZI Over the SPI and SPEI

3.2.1. The Relationship Between Hydrological Data and Multiscalar Drought Indices

Previous work has shown that hydrological variables can serve as good indicators of drought and have exhibited strong relationships with drought indices at different timescales [*Vicente-Serrano and López-Moreno*, 2005; *McEvoy et al.*, 2012]. To gain a better understanding of the performance of the SZI, SPEI, and SPI, the correlations between observed streamflow and moisture availability identified by different multiscalar

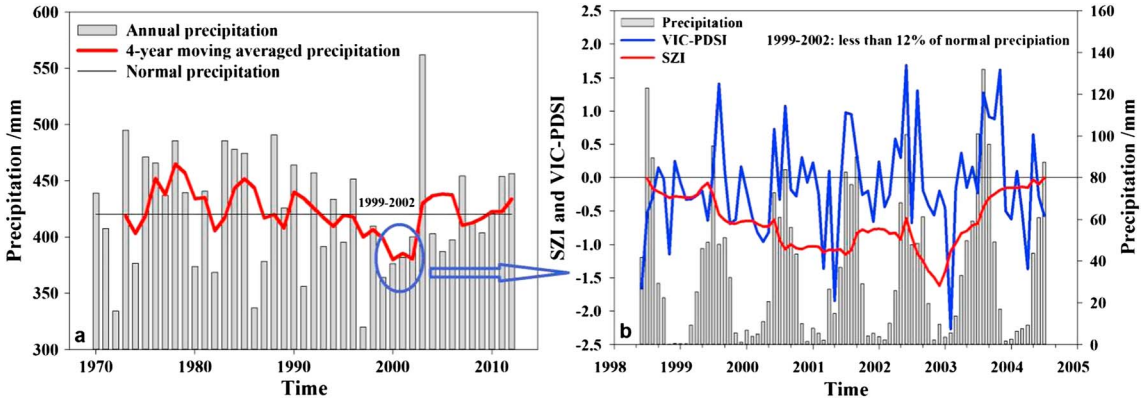

Figure 5. (a) Time series of annual precipitation and 4 year moving average precipitation during the period of 1971–2012 and (b) time series of VIC-PDSI, 48 month SZI, and monthly precipitation during 1999–2002 on the Loess Plateau.

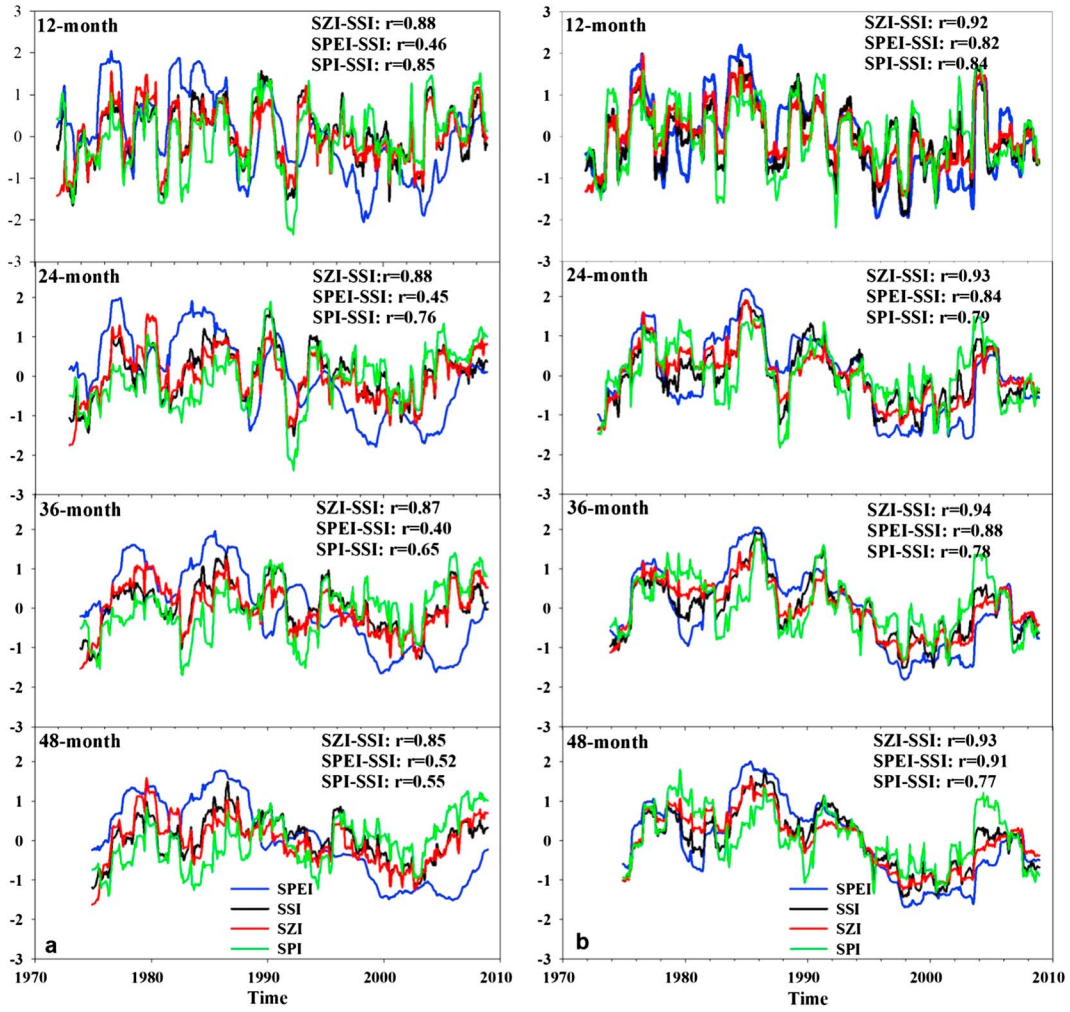

Figure 6. The Standardized Streamflow Index (SSI) and spatially averaged SZI, SPEI, and SPI from corresponding watershed grid cells at (a) Hongqi and (b) Huaxian for 12, 24, 36, and 48 months.

drought indices were examined and evaluated. Each drought index was calculated following the same procedure. Due to the log-logistic distribution used to calculate the SZI, SPEI, and SPI, we also chose this probability distribution to standardize the observed streamflow data to get the Standardized Streamflow Index (SSI) [*Vicente-Serrano et al*., 2014]. The aim of calculating the Pearson correlation coefficients between drought indices and streamflow at certain timescales is to evaluate which drought index has the best performance in drought identification under the same conditions. Figure 6 illustrates the SSI and spatially averaged SZI, SPEI, and SPI from the watershed grid cells for Hongqi and Huaxian at different timescales. All drought indices appear to detect the major drought periods in Hongqi and Huaxian according to the observed streamflow data. However, the Pearson correlation coefficients of the SZI-SSI at Hongqi station are 0.88, 0.88, 0.87, and 0.85 at the 12, 24, 36, and 48 month scale, respectively, which are apparently higher than those for the SPEI-SSI (ranging from 0.40 to 0.52) and SPI-SSI (ranging from 0.55 to 0.85). Similarly, the Pearson correlation coefficients between the SZI and SSI at Huaxian station, which range from 0.92 to 0.94, are also higher than those for the SPEI (0.82–0.91) and SPI (0.77–0.84). Therefore, it is evident that the errors of the SZI are lowest among the three multiscalar drought indices at each timescale and location, demonstrating that the SZI provides improved information for drought monitoring.

3.2.2. The Relationship Between the Vegetation Index and Drought Indices

We also evaluated the SZI, SPI, and SPEI with the NDVI over the six subregions in the Loess Plateau. The Pearson correlation coefficients between the annual mean NDVI and the December 12 month scale drought indices were calculated with correlation analysis (Table 2). It should be noted that the Pearson correlation

Table 2. The Pearson Correlation Coefficients (*r*) Between December 12 Month SPI, SPEI, and SZI and Annual Mean NDVI (1982–2006) Over Six Subregions of the Loess Plateau

Subregion	SPI	SPEI	SZI
1	0.50*	0.44*	0.51*
2	0.48*	0.42*	0.56**
3	0.40	0.44*	0.54*
4	0.63**	0.67**	0.73**
5	0.67**	0.60**	0.76**
6	0.66**	0.61**	0.68**

*Significant at the 95% confidence level.
**Significant at the 99% confidence level.

coefficients between the NDVI and drought indices vary with the climatic region, which can be attributed to each subregion of the Loess Plateau having a different sensitivity to moisture availability. However, it is clear that the Pearson correlation coefficients between the SZI and the NDVI range between 0.51 and 0.76, which are higher than those for the SPEI and the NDVI (0.42–0.67) and for the SPI and the NDVI (0.40–0.67) in all subregions. The above analysis indicates that the SZI performs the best among the three multiscalar drought indices in reflecting vegetation changes.

In addition, based on the time series shown in Figure 4, two specific drought events, one in November 1997 and the other in July 2000, were selected to further characterize the correlation between the NDVI and the SZI, SPEI, and SPI. As shown in Figure 7, the spatial patterns of the 12 month scale drought episode in November 1997 are identified by the SZI, SPEI, and SPI. However, the drought severity differs; the drought level characterized by the SPEI is much more severe than that of the SZI or SPI. The correlation coefficient between the SZI and NDVI is 0.51, which is higher than that of SPEI-NDVI (0.28) or SPI-NDVI (0.43). Therefore, it is clear that the spatial pattern of the NDVI anomaly is more comparable with that of the SZI than with that of the SPEI or SPI. During the 12 month period from December 1996 to November 1997, the precipitation was

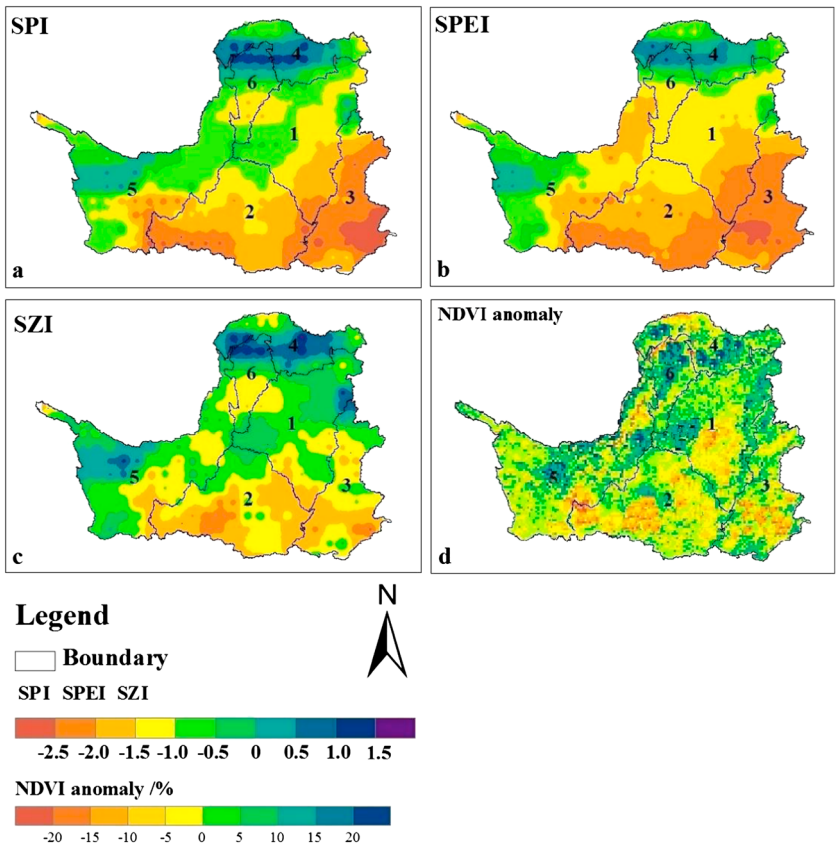

Figure 7. The spatial distribution of the 12 month SPI, SPEI, SZI, and NDVI anomaly percentile (relative to 1982–2006) in November 1997.

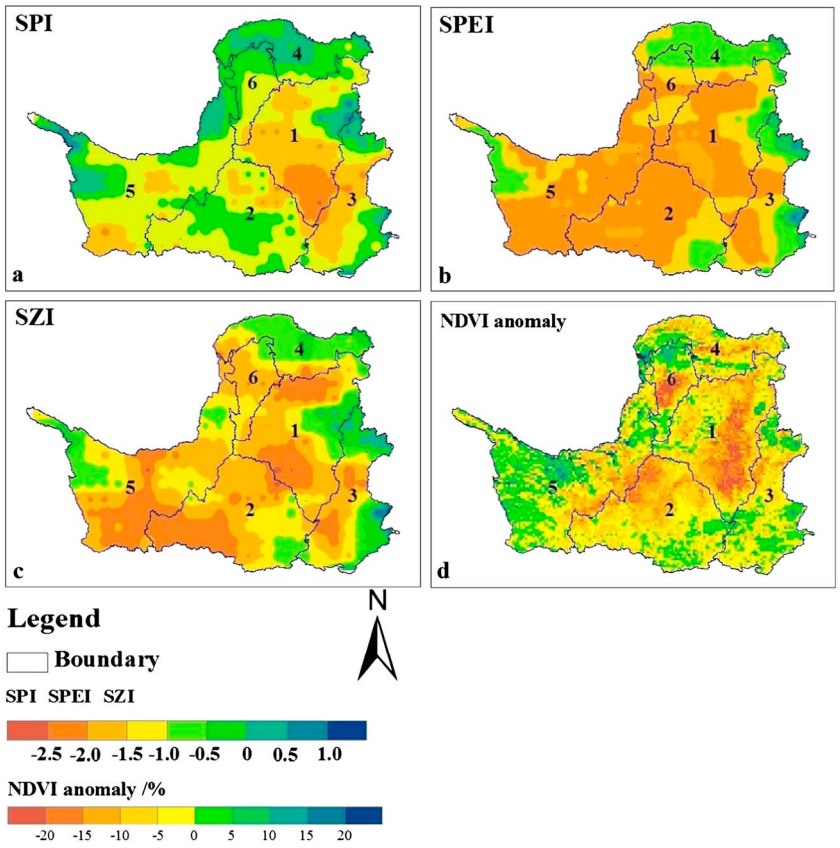

Figure 8. The spatial distribution of the 12 month SPI, SPEI, SZI, and NDVI anomaly percentile (relative to 1982–2006) in July 2000.

104.3 mm lower than the total annual average over the entire study period. The mean $\widehat{P}$ was 1.4% above the average over this period, but the PE was 5.8% above the average over the same period. As we have discussed, $\widehat{P}$ in the SZI considers evapotranspiration, runoff, and any changes in soil moisture storage in estimating the water demand [*Palmer*, 1965], while PE in the SPEI is the only variable used to quantify such a demand. Thus, we can clearly see that the SPEI has a lower correlation coefficient with the NDVI anomaly when compared with the SZI (Figure 7).

Figure 8 exhibits the spatial distribution of the 12 month SZI, SPEI, and SPI in July 2000, where the spatial patterns characterized by the three multiscalar drought indices are in accordance with each other, but the severity is different. The drought severity identified by the SZI and SPEI is higher than that of the SPI. The correlation coefficients of SZI-NDVI and SPEI-NDVI are 0.46 and 0.44, respectively, which are higher than that of SPI-NDVI (0.31). The spatial pattern of the NDVI anomaly is more comparable with that of the SZI and SPEI than with that of the SPI. The total precipitation amount from August 1999 to July 2000 was 103.9 mm lower than the total annual average over the entire study period. We found that the mean PE and $\widehat{P}$ for this period were 4.4% and 3.1% above average, respectively. As a result, both lower precipitation and higher water demand are the main reasons for the drought in July 2000. The inclusion of water demand in the SZI and SPEI enables these indices to better quantify the drought. However, the SPI, which is based simply on precipitation without considering water demand, has the lowest correlation with the NDVI.

4. Conclusions

In this study, we have described a physically based multiscalar drought index, SZI, which uses the moisture anomaly index as an indicator of surface water balance and drought conditions. The water budget accounting in the SZI is based on the hydrological processes simulated by the VIC model, and the other calculation procedures of the SZI follow those of the SPEI. The SZI is quantitatively compared with VIC-PDSI and the two most widely used multiscalar drought indices, the SPI and SPEI.

The SZI has a multiscalar advantage over the VIC-PDSI, which is important in monitoring the severity and duration of droughts at different timescales. The SZI agrees better with the observed changes in the streamflow and vegetation index than the SPEI or the SPI, indicating that the SZI performs better than the SPI or SPEI in identifying drought events at different timescales. The SPI depends only on precipitation and ignores other components of the surface water balance equation that can lead to increased drought severity. In the calculation of the SZI, $\widehat{P}$ includes precipitation, soil moisture loss and recharge, runoff, and evapotranspiration, and all these variables can affect surface water balance and thus drought conditions, whereas PE considers only atmospheric demand for water. Such a strategy makes the SZI physically more reasonable and reliable. With respect to actual water demand and the multiscalar characteristic of drought, the SZI provides better information for drought monitoring and identification at various temporal scales.

The main limitation of the SZI is that its computation is more complex and difficult than the computation of the SPI and the SPEI. To facilitate the use of the SZI for interested researchers, our computer programs and data related to the calculation of the SZI will be voluntarily provided. Given the opportunity, we would like to collaborate with agencies such as the China Meteorological Administration to add our drought index, SZI, into their drought prediction systems, as this will be of great benefit for our research, the agencies, and water managers. Another limitation of the SZI is that its calculation requires long-term climatic and hydrologic records, which makes it unsuitable for short-term drought identification. Despite such limitations, our newly developed drought index more realistically characterizes the variability of dry and wet spells when compared with some of the other existing drought indices and provides a better tool for monitoring water resources. Further validation of the SZI will be performed at the global scale.

Acknowledgments

The meteorological forcing data for calculating the drought indices are available at the Data and Information Center of the China Meteorological Administration (http://data.cma.gov.cn/site/index.html). The DEM data set was obtained from the advanced spaceborne thermal emission and reflection radiometer global digital elevation model (http://gdem.ersdac.jspacesystems.or.jp). The NDVI data are available at the NOAA advanced very high resolution radiometer land data set (http://glcf.umd.edu/data/). The observed hydrologic data are from the Hydrology Bureau of the Yellow River Conservancy Commission of China (http://www.hwswj.gov.cn/swjcms/index.jsp). The CPC soil moisture data set was downloaded from Earth System Research Laboratory (http://www.esrl.noaa.gov/psd/data/gridded/data.cpcsoil.html). This work is jointly supported by the National Science and Technology Supporting Plan (2011BAD29B09), the National Natural Science Foundation of China (41530752), and the Fundamental Research Funds for the Central Universities (lzujbky-2015-152). Three reviewers are thanked for their constructive comments, which substantially improved the manuscript. These authors Baoqing Zhang and Xining Zhao contributed equally to this work.

References

Allen, R. G., L. S. Pereira, D. Raes, and M. Smith (1998), Crop evapotranspiration, guidelines for computing crop water requirements, 300 pp., FAO Irrig. and Drain. Paper 56, Food and Agric. Orgn. of the United Nations, Rome, Italy.

Alley, W. M. (1984), The Palmer Drought Severity Index: Limitations and assumptions, *J. Climate Appl. Meteorol.*, *23*(7), 1100–1109, doi:10.1175/1520-0450(1984)023<1100:tpdsil>2.0.co;2.

Brocca, L., F. Melone, T. Moramarco, and R. Morbidelli (2010), Spatial-temporal variability of soil moisture and its estimation across scales, *Water Resour. Res.*, *46*, W02516, doi:10.1029/2009WR008016.

Brocca, L., L. Ciabatta, C. Massari, T. Moramarco, S. Hahn, S. Hasenauer, R. Kidd, W. Dorigo, W. Wagner, and V. Levizzani (2014), Soil as a natural rain gauge: Estimating global rainfall from satellite soil moisture data, *J. Geophys. Res. Atmos.*, *119*, 5128–5141, doi:10.1002/2014JD021489.

Carbone, G. J., J. Rhee, H. P. Mizzell, and R. Boyles (2008), A regional-scale drought monitoring tool for the Carolinas, *Bull. Am. Meteorol. Soc.*, *89*, 20–28, doi:10.1175/BAMS-89-1-20.

Dai, A. G. (2011), Characteristics and trends in various forms of the Palmer Drought Severity Index during 1900–2008, *J. Geophys. Res.*, *116*, D12115, doi:10.1029/2010JD015541.

Dai, A. G. (2013), Increasing drought under global warming in observations and models, *Nat. Clim. Change*, *3*, 52–58, doi:10.1038/NCLIMATE1633.

Dai, A. G., K. E. Trenberth, and T. T. Qian (2004), A global dataset of Palmer Drought Severity Index for 1870–2002: Relationship with soil moisture and effects of surface warming, *J. Hydrometeorol.*, *5*(6), 1117–1130, doi:10.1175/JHM-386.1.

Dan, L., J. Ji, Z. H. Xie, F. Chen, G. Wen, and J. E. Richey (2012), Hydrological projections of climate change scenarios over the 3H region of China: A VIC model assessment, *J. Geophys. Res.*, *117*, D11102, doi:10.1029/2011JD017131.

Hansen, M. C., R. S. Defries, J. R. G. Townshend, and R. Sohlberg (2000), Global land cover classification at 1 km spatial resolution using a classification tree approach, *Int. J. Remote Sens.*, *21*, 1331–1364, doi:10.1080/014311600210209.

Hao, Z. C., and A. AghaKouchak (2013), Multivariate standardized drought index: A parametric multi-index model, *Adv. Water Resour.*, *57*, 12–18, doi:10.1016/j.advwatres.2013.03.009.

Hayes, M., D. A. Wilhite, M. Svoboda, and O. Vanyarkho (1999), Monitoring the 1996 drought using the Standardized Precipitation Index, *Bull. Am. Meteorol. Soc.*, *80*, 429–438, doi:10.1175/1520-0477(1999)080<0429:MTDUTS>2.0.CO;2.

Liang, X., D. P. Lettenmaier, E. F. Wood, and S. J. Burges (1994), A simple hydrologically based model of land-surface water and energy fluxes for general-circulation models, *J. Geophys. Res.*, *99*(D7), 14,415–14,428, doi:10.1029/94JD00483.

McEvoy, D. J., J. L. Huntington, J. T. Abatzoglou, and L. M. Edwards (2012), An evaluation of multiscalar drought indices in Nevada and Eastern California, *Earth Interact.*, *16*, 1–18, doi:10.1175/2012EI000447.1.

McKee, T. B., N. J. Doesken, and J. Kleist (1993), The relationship of drought frequency and duration to time scales, in *Proceedings of the 8th Conference of Applied Climatology*, pp. 179–184, Am. Meteorol. Soc., Boston, Mass.

Mishra, A. K., and V. P. Singh (2010), A review of drought concepts, *J. Hydrol.*, *391*(1–2), 202–216, doi:10.1016/j.jhydrol.2010.07.012.

Mishra, A. K., A. V. M. Ines, N. N. Das, C. P. Khedun, V. P. Singh, B. Sivakumar, and J. W. Hansen (2015), Anatomy of a local-scale drought: Application of assimilated remote sensing products, crop model, and statistical methods to an agricultural drought study, *J. Hydrol.*, *526*, 15–29, doi:10.1016/j.jhydrol.2014.10.038.

Mu, Q. Z., M. S. Zhao, J. S. Kimball, N. G. McDowell, and S. W. Running (2013), A remotely sensed global terrestrial drought severity index, *Bull. Am. Meteorol. Soc.*, *94*, 83–98, doi:10.1175/BAMS-D-11-00213.1.

Myneni, R. B., J. Dong, C. J. Tucker, R. K. Kaufmann, P. E. Kauppi, J. Liski, L. Zhou, V. Alexeyev, and M. K. Hughes (2001), A large carbon sink in the woody biomass of Northern forests, *Proc. Natl. Acad. Sci. U.S.A.*, *98*, 14,784–14,789, doi:10.1073/pnas.261555198.

Nash, J. E., and J. Sutcliffe (1970), River flow forecasting through conceptual models: Part 1—A discussion of principles, *J. Hydrol.*, *10*, 282–290.

Palmer, W. C. (1965), *Meteorological Drought*, *Res. Pap.*, vol. 45, 58 pp., U.S. Weather Bureau, Washington, D. C.

Prigent, C., F. Aires, W. B. Rossow, and A. Robock (2005), Sensitivity of satellite microwave and infrared observations to soil moisture at a global scale: Relationship of satellite observations to in situ soil moisture measurements, *J. Geophys. Res.*, *110*, D07110, doi:10.1029/2004JD005087.

Rajsekhar, D., V. P. Singh, and A. K. Mishra (2015), Multivariate drought index: An information theory based approach for integrated drought assessment, *J. Hydrol.*, *526*, 164–182, doi:10.1016/j.jhydrol.2014.11.031.

Reynolds, C. A., T. J. Jackson, and W. J. Rawls (2000), Estimating soil water holding capacities by linking the Food and Agriculture Organization soil map of the world with global pedon databases and continuous pedotransfer functions, *Water Resour. Res.*, *36*(12), 3653–3662, doi:10.1029/2000WR900130.

Sheffield, J., and E. F. Wood (2007), Characteristics of global and regional drought, 1950–2000: Analysis of soil moisture data from off-line simulation of the terrestrial hydrologic cycle, *J. Geophys. Res.*, *112*, D17115, doi:10.1029/2006JD008288.

Sheffield, J., G. Goteti, F. H. Wen, and E. F. Wood (2004), A simulated soil moisture based drought analysis for the United States, *J. Geophys. Res.*, *109*, D24108, doi:10.1029/2004JD005182.

Shi, W. J., F. L. Tao, J. Y. Liu, X. L. Xu, W. H. Kuang, J. W. Dong, and X. L. Shi (2014), Has climate change driven spatio-temporal changes of cropland in northern China since the 1970s?, *Clim. Change*, *124*, 163–177, doi:10.1007/s10584-014-1088-1.

Todd, B., N. Macdonald, R. C. Chiverrell, C. Caminade, and J. M. Hooke (2013), Severity, duration and frequency of drought in SE England from 1697 to 2011, *Clim. Change*, *121*, 673–687, doi:10.1007/s10584-013-0970-6.

Tucker, C. J., J. E. Pinzon, M. E. Brown, D. A. Slayback, E. W. Pak, and R. Mahoney (2005), An extended AVHRR 8-km NDVI data set compatible with MODIS and SPOT vegetation NDVI data, *Int. J. Remote Sens.*, *26*(20), 4485–4498, doi:10.1080/01431160500168686.

Vicente-Serrano, S. M., and J. I. López-Moreno (2005), Hydrological response to different time scales of climatological drought: An evaluation of the Standardized Precipitation Index in a mountainous Mediterranean basin, *Hydrol. Earth Syst. Sci.*, *9*(5), 523–533, doi:10.5194/hess-9-523-2005.

Vicente-Serrano, S. M., S. Beguería, and J. I. López-Moreno (2010), A multiscalar drought index sensitive to global warming: The Standardized Precipitation Evapotranspiration Index, *J. Clim.*, *23*(7), 1696–1718, doi:10.1175/2009JCLI2909.1.

Vicente-Serrano, S. M., J. I. López-Moreno, L. Gimeno, R. Nieto, E. Morán-Tejeda, J. Lorenzo-Lacruz, and S. Beguería (2011), A multiscalar global evaluation of the impact of ENSO on droughts, *J. Geophys. Res.*, *116*, D20109, doi:10.1029/2011JD016039.

Vicente-Serrano, S. M., S. Beguería, and J. I. López-Moreno (2012), Comment on "Characteristics and trends in various forms of the Palmer Drought Severity Index (PDSI) during 1900–2008" by Aiguo Dai, *J. Geophys. Res.*, *116*, D19112, doi:10.1029/2011JD016410.

Vicente-Serrano, S. M., et al. (2014), Evidence of increasing drought severity caused by temperature rise in southern Europe, *Environ. Res. Lett.*, *9*, 044001, doi:10.1088/1748-9326/9/4/044001.

Wang, A. H., T. J. Bohn, S. P. Mahanama, R. D. Koster, and D. P. Lettenmaier (2009), Multimodel ensemble reconstruction of drought over the continental United States, *J. Clim.*, *22*(10), 2694–2712, doi:10.1175/2008JCLI2586.1.

Wang, A. H., D. P. Lettenmaier, and J. Sheffield (2011), Soil moisture drought in China, 1950–2006, *J. Clim.*, *24*(13), 3257–3271, doi:10.1175/2011JCLI3733.1.

Wang, G. Q., J. Y. Zhang, J. L. Jin, T. C. Pagano, R. Calow, Z. X. Bao, C. S. Liu, Y. L. Liu, and X. L. Yan (2012), Assessing water resources in China using PRECIS projections and a VIC model, *Hydrol. Earth Syst. Sci.*, *16*(1), 231–240, doi:10.5194/hess-16-231-2012.

Wang, Y. Q., M. A. Shao, Y. J. Zhu, and Z. P. Liu (2011), Impacts of land use and plant characteristics on dried soil layers in different climatic regions on the Loess Plateau of China, *Agric. For. Meteorol.*, *151*, 437–448, doi:10.1016/j.agrformet.2010.11.016.

Wells, N., S. Goddard, and M. J. Hayes (2004), A self-calibrating Palmer Drought Severity Index, *J. Clim.*, *17*, 2335–2351, doi:10.1175/1520-0442(2004)017<2335:ASPDSI>2.0.CO;2.

Wilhite, D. A. (2000), Drought as a natural hazard: Concepts and definitions, in *Droughts: A Global Assessment*, edited by D. A. Wilhite, pp. 3–18, Routledge, New York.

Wu, Z. Y., G. H. Lu, L. Wen, C. A. Lin, J. Y. Zhang, and Y. Yang (2007), Thirty-five year (1971–2005) simulation of daily soil moisture using the variable infiltration capacity model over China, *Atmos. Ocean*, *45*(1), 37–45, doi:10.3137/ao.v450103.

Wu, Z. Y., G. H. Lu, L. Wen, and C. A. Lin (2011), Reconstructing and analyzing China's fifty-nine year (1951–2009) drought history using hydrological model simulation, *Hydrol. Earth Syst. Sci.*, *15*, 2881–2894, doi:10.5194/hess-15-2881-2011.

Xie, Z. H., F. Yuan, Q. Y. Duan, J. Zheng, M. L. Liang, and F. Chen (2007), Regional parameter estimation of the VIC land surface model: Methodology and application to river basins in China, *J. Hydrometeorol.*, *8*(3), 447–468, doi:10.1175/JHM568.1.

Xin, Z. B., X. X. Yu, Q. Y. Li, and X. X. Lu (2011), Spatiotemporal variation in rainfall erosivity on the Chinese Loess Plateau during the period 1956–2008, *Reg. Environ. Change*, *11*(1), 149–159, doi:10.1007/s10113-010-0127-3.

Xu, J., L. L. Ren, X. H. Ruan, X. F. Liu, and F. Yuan (2012), Development of a physically based PDSI and its application for assessing the vegetation response to drought in northern China, *J. Geophys. Res.*, *117*, D08106, doi:10.1029/2011JD016807.

Yan, Y. X., and J. X. Xu (2007), A study of scale effect on specific sediment yield in the Loess Plateau, China, *Sci. China Earth Sci.*, *50*(1), 102–112, doi:10.1007/s11430-007-2024-2.

Yuan, S., and S. M. Quiring (2014), Drought in the U.S. Great Plains (1980–2012): A sensitivity study using different methods for estimating potential evapotranspiration in the Palmer Drought Severity Index, *J. Geophys. Res. Atmos.*, *119*, 10,996–11,010, doi:10.1002/2014JD021970.

Zhai, J., B. Su, V. Krysanova, T. Vetter, C. Gao, and T. Jiang (2010), Spatial variation and trends in PDSI and SPI indices and their relation to streamflow in 10 large regions of China, *J. Clim.*, *23*, 649–663, doi:10.1175/2009JCLI2968.1.

Zhai, P. M., X. B. Zhang, H. Wan, and X. H. Pan (2005), Trends in total precipitation and frequency of daily precipitation extremes over China, *J. Clim.*, *18*, 1096–1108, doi:10.1175/JCLI-3318.1.

Zhang, B. Q., P. T. Wu, X. N. Zhao, Y. B. Wang, J. W. Wang, and Y. G. Shi (2012), Drought variation trends in different subregions of the Chinese Loess Plateau over the past four decades, *Agric. Water Manage.*, *115*, 167–177, doi:10.1016/j.agwat.2012.09.004.

Zhang, B. Q., P. T. Wu, X. N. Zhao, Y. B. Wang, and X. D. Gao (2013), Changes in vegetation condition in areas with different gradients (1980–2010) on the Loess Plateau, China, *Environ. Earth Sci.*, *68*, 2427–2438, doi:10.1007/s12665-012-1927-1.

Zhang, B. Q., P. T. Wu, X. N. Zhao, and X. D. Gao (2014), Spatiotemporal analysis of climate variability (1971–2010) in spring and summer on the Loess Plateau, China, *Hydrol. Processes*, *28*(4), 1689–1702, doi:10.1002/hyp.9724.

Zou, X. K., P. M. Zhai, and Q. Zhang (2005), Variations in droughts over China: 1951–2003, *Geophys. Res. Lett.*, *32*, L04707, doi:10.1029/2004GL021853.